doi:10.2533/chimia.2024.339 Chimia 78 (2024) 339–343

Quasi-operando Transmission Electron Microscopy Diagnostics for Electrocatalytic Processes in Liquids

Vasiliki Tileli*

Abstract: It is of great interest to the energy community to understand how the mechano-physico-chemical phenomena that eventually lead to device degradation are related to the startup, operation, and shutdown phases. For electrocatalytic systems operating in liquid electrolyte environments, the understanding of these phenomena at each stage can pave the way for the tailored design of efficient and commercially viable electrocatalysts. Transmission electron microscopy plays an important role in the investigation of local electrocatalytic effects, complementing other *operando* characterization techniques. Herein, after attempting to define the meaning of *operando* methodologies in relation to electron microscopy studies, the progress in the field is reviewed in terms of the knowledge gained about the catalysts, the solid-liquid interfaces, and the solid-liquid-gas interfacial phenomena for several electrocatalytic reactions. Finally, the parameters that require consideration in *quasi-operando* ec-LPTEM studies of electrocatalytic systems are discussed.

Keywords: Electrocatalysis · Liquid-phase · *Operando* · Transmission electron microscopy

1. Introduction

The real-time monitoring and manipulation of solid-liquid interfaces in catalytic materials under changes induced by the application of voltage is considered to be of critical importance to the energy community.[1] In particular, with respect to heterogeneous metal and metal-oxide catalytic systems,[2,3] insights into the processes that take place during reactions including oxygen evolution, oxygen reduction, CO_2 reduction, hydrogen evolution, and nitrate reduction (OER, ORR, CO_2ER, HER, and NRR) can pave the way for the design of efficient electrocatalytic systems that can contribute to the urgent challenge of keeping our planet afloat by relying entirely on sustainable energy sources and eventually eliminating fossil fuels. This need has led to important advances in *operando* characterization techniques, with X-ray and optical spectroscopies leading the way in their application to catalytic systems.[4-6] Based on these experiments, about 20 years ago, Miguel A. Bañares introduced protocols regarding the terminology associated with *operando* methodologies.[7] He stated that for a measurement to be described as *operando*, the real-time acquisition of data relating to a property, such as stability information in the native environment of the process, must be accompanied by simultaneous activity (and/or selectivity) measurements of the catalytic systems under investigation. In recent years, electrochemical liquid-phase transmission electron microscopy (ec-LPTEM) has become increasingly popular for the real-time study of electrocatalytic phenomena, due to the availability of commercial equipment and miniaturized cells that allow the study of catalysts with an abundance of acquired signals.[8,9] Although many articles have been published, the use of the term *operando* is a grey area when referring to EM-based studies, and is sometimes used loosely. This is because, unlike X-ray and other spectroscopies, activity measurements in TEM microcells that contain liquids, are not possible *a priori*, at least at the time of publication of this perspective and for the foreseeable future. Therefore, this review will first attempt to provide a framework for the concept of *operando* as it can be applied to EM-studies, prior to revisiting the results that have already been obtained using ec-LPTEM applied to electrocatalytic systems in liquids and that can be considered *operando*.

2. On the Term *Operando* in Electron Microscopy Diagnostics of Electrocatalysts

Activity or selectivity measurements of catalysts in electrocatalysis laboratories are carried out in dedicated cells where conditions are well controlled in each experiment. For example, a common way to evaluate the activities of metal-oxide particles for oxygen electrocatalysis is to use the rotating disc electrode (RDE) cell, Fig. 1a. This three-electrode electrochemical cell, described in detail previously,[10] includes a working electrode (WE), which is typically inert to the reaction of interest, a counter electrode (CE), which is chosen to promote the reaction at the WE, and a reference electrode (RE), which is used to calibrate the potential and needs to remain chemically intact during the process. Fig. 1b shows the WE (grey interior), where a compact layer consisting of the catalyst powder, a binder and carbon black is deposited to establish electrochemical contact between the catalyst and the electrode. In this configuration, the disc substrate electrode is a few millimeters (of the order of 3 mm) and the loading of the catalyst ink is such that it forms a thick layer (as seen in the cross-sectional schematic of Fig. 1c) and thus overtakes the current response of the substrate electrode. The ability to perform quantitative activity measurements lies in the determination of the electrochemical surface area (ESCA), which allows the conversion of the current measured by cyclic voltammetry or galvanostatic hold to current density. Methods for calculating the ESCA have been detailed in Trassati and Petrii.[11] On the other hand, the microcells developed for liquid-phase TEM studies[12] have a completely different configuration, mainly due to the volume constraints that have to do with their insertion into the TEM polepiece. Fig. 1d depicts the co-planar configuration of the three-electrode TEM microcell system, where typically only the WE is in the field of view of real-time electron imaging. The electrochemically active surface area of the WE is restricted to a small area with the addition of

*Correspondence: Dr. V. Tileli, E-mail: vasiliki.tileli@epfl.ch
Institute of Materials, École Polytechnique Fédérale de Lausanne, CH–1015 Lausanne, Switzerland

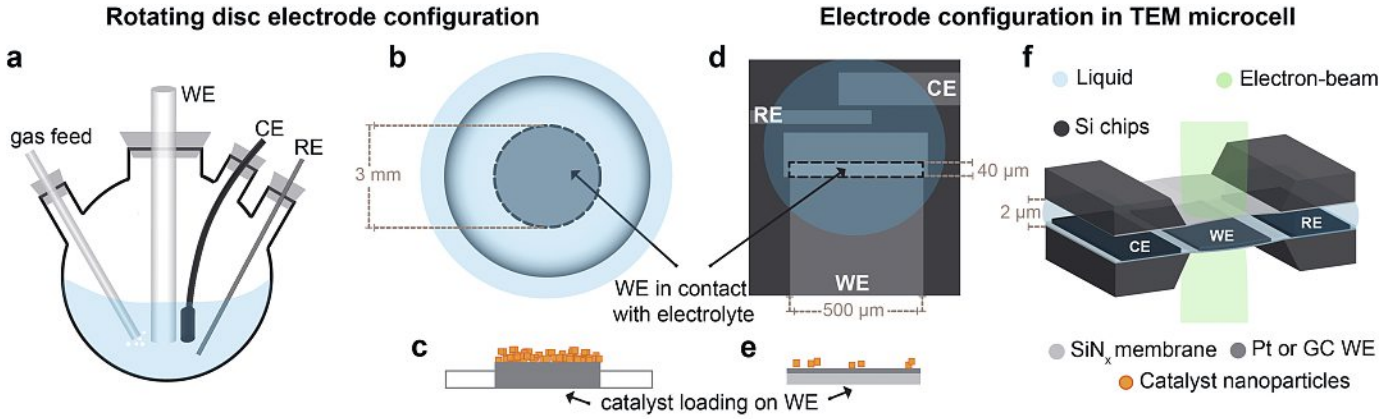

Fig. 1. (a) Schematic depicting the configuration of the RDE setup for catalyst activity measurements, (b) top-down view of the area corresponding to the bare working electrode surface (grey disc) in contact with the electrolyte (in light blue), and (c) cross-sectional view of the catalyst loading on the working electrode. (d) Top-down view of the electrochemical TEM chip showing the area of the working electrode that is exposed to the electrolyte and (e) cross-sectional view of its catalyst loading. (f) Overview illustration of the TEM microcell used to perform electrochemical experiments. The schematics are not-to-scale and the dimensions given are indicative.

an insulating passivation layer. The area of the substrate working electrode that participates in the reaction is of the order of a few hundred of µm^2, where the pure catalyst (or catalyst ink) is deposited by dropcasting with a loading that is typically much less than a monolayer (Fig. 1e), as allowed by the vertical dimensions (a couple of µm max, Fig. 1f) and as imposed by the ability to image in transmission or scanning transmission mode. Thus, the calculation of ESCA mainly involves the area of the substrate electrode participating in the reaction and not the area of the deposited catalyst particles, which is small and difficult to assess accurately. Therefore, the current density calculations cannot reflect the properties of the catalysts.

Hence, according to the definition by Bañares, the term *operando* is rendered unusable for TEM diagnostics of electrocatalysts in liquids since they cannot be directly related to activity. At the same time, *operando* etymologically refers to 'action', *i.e.* during operation. Hitherto, for TEM studies that can be applied to electrochemical processes that are monitored continuously from start to finish, during operation, a more appropriate term may be *quasi-operando*, *i.e.* almost *operando*. Otherwise, if the catalysts cannot be imaged throughout the application of the electrochemical potential, but only in parts, then the methodology can be described as *in situ*, *i.e.* in location. On the basis of this distinction, this review is dedicated exclusively to studies reporting on the evolution of the catalytic system as imaged or probed by TEM methodologies, when the evolution is followed for the totality of the electrocatalytic process that is induced by the application of bias through electrodes (and not the electron beam). It should be noted that this is irrespective of whether the term *operando* appears in the title or in the main text of published articles.

3. Aspects of *Quasi-operando* Electrocatalytic Diagnostics with ec-LPTEM

Electron imaging, diffraction, and spectroscopy have all been realized in *quasi-operando* mode for catalyst evolution studies in liquid-phase TEM. The investigations concern transformations related to the morphology and/or structure of the solid catalysts, the solid/liquid interactions, and the solid/liquid/gas interactions. Fig. 2 compares the implementation of *quasi-operando* ec-LPTEM on OER, ORR, CO_2ER, and HER catalytic systems and summarizes the main results, which are described below.

3.1 *Catalyst (Solid) Evolution*

As the radar plot in Fig. 2a shows, ec-LPTEM has primarily provided insight into the evolution of electrocatalysts in terms of their morphological and structural changes, while being implemented for a wide range of reactions over the entire pH range of electrolytes.

3.1.1 *Morphological and Structural Analysis of OER Catalysts*

OER in alkaline environment (0.1 M KOH, pH 13) in the TEM was first reported by Pena *et al.* in a study that used spinel Co_3O_4 nanocatalysts to investigate morphological changes under OER-like conditions.[13] The authors performed a series of control experiments where it was shown that cyclic voltammetry (CV) measurements in a three-electrode system exhibited a drift in the potential scale with time. Instead, the *operando* acquisition was performed using chronopotentiometry (CP) which showed an irreversible and extended amorphization matrix of the metal-oxide catalysts after the first two minutes. The image transformation was attributed to the oxyhydroxide phase formation. Cobalt oxides were also used for the OER study by Shen *et al.* where their electrochemical response was imaged in a customized three-electrode system under CV measurements between 1.0 V and 1.8 V against the reversible hydrogen electrode (RHE) at pH 13.[14] In this work, no visible morphological changes were observed during the first 15 cycles. *Operando* structural analysis using electron diffraction of $Ba_{0.5}Sr_{0.5}Co_{0.8}Fe_{0.2}O_{3-\delta}$ particles showed that the bulk perovskite core remained stable, while the surface spinel reflections redistributed during cycling, revealing a rotation of the surface atomic positions *via* a surface reconstruction mechanism. Finally, Balaghi *et al*. performed ec-LPTEM experiments in a copper complex using phosphate buffer as the electrolyte (pH 7).[15] The spatial resolution inhibited the imaging on the working electrode, while reprecipitated particles were seen to form outside the electrode area, an insulating region that does not experience the reaction potential. The authors also reported the structural transformation of the copper complex to the copper (II) oxide as revealed by electron diffraction experiments.

Overall, morphological changes of OER catalysts are subtle effects that are difficult to monitor in detail in the case of the time-limited experiments carried out by ec-LPTEM.

3.1.2 *Morphological Evolution in Pt-based ORR Catalysts*

One of the first experiments performed with ec-LPTEM in catalytic systems was reported 10 years ago with the advent of the mainstream TEM add-on equipment. The study involved the simultaneous electron imaging and CV measurements of Pt-Fe nanoparticles on carbon supports in perchloric acid (pH 1.1).[16]

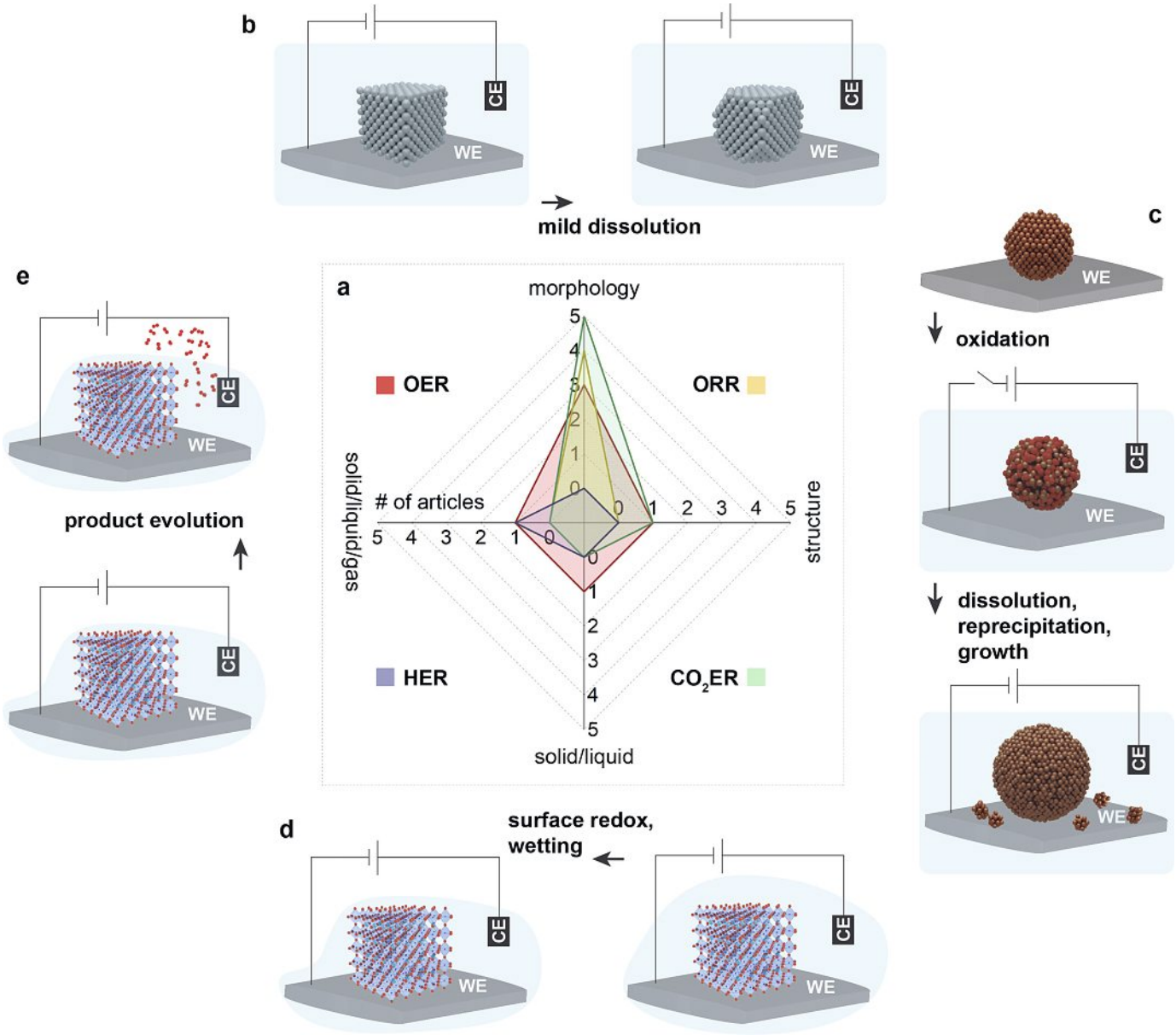

Fig. 2. Comparative overview of the implementation of *quasi-operando* ec-LPTEM for electrocatalytic systems. (a) Radar plot separating the published contributions of *quasi-operando* TEM in terms of the morphology, structure, solid/liquid, and solid/liquid/gas insights for ORR, CO_2ER, HER, and OER. (b-e) Simplified schematics depicting the imaged/probed transformations of (b) noble metals (Pt nanocubes) under ORR, (c) non-noble metals (Cu nanospheres) under CO_2ER, and oxides (perovskite nanoparticles) under OER for (d) wetting and (e) product evolution phenomena.

Therein, Zhu *et al.* used a two-electrode configuration system and absolute voltage values were reported as no reference electrode was used to calibrate the voltage. Additionally, the recorded 100 cycles showed unexpected, large variations in the CV curves and therefore the interpretation of the dissolution/reprecipitation of the nanocatalysts that was evident in the TEM recorded images was difficult to relate directly to the electrochemical stimuli. In a very similar approach, Beermann *et al*. investigated Pt-Ni catalysts on carbon supports at acidic conditions, where this time they performed CV cycling with a calibrated potential for up to 20 cycles and included holds at upper potentials.[17] The authors reported the calibrated potential as a function of time profiles, but the *operando* CV curves were not reported. The authors concluded that Ni-rich particles would dissolve during catalyst activation and that the Pt-Ni particles tended to aggregate at extreme upper potentials. In the same lines, Shen *et al*. performed CV measurements with a three-electrode system in model, free-standing Pt nanocube catalysts at pH 1.1.[18] The authors were able to maintain a stable CV response for 350 cycles by low-dose electron imaging in transmission mode using a direct electron detection camera. Their results showed that the nanocube catalysts remained stable for 150 cycles, after which subtle Pt dissolution (Fig. 2b) began and further aging resulted in merging of the structures. Finally, in a different approach, Impagnatiello *et al*. deposited an ink containing the entire cathode side of a proton exchange membrane fuel cell with the Pt nanoparticles, the carbon support and the ionomer network on the TEM electrochemical chip.[19] Using the same acidic electrolyte, they performed up to 500 CVs, adjusting the electron beam conditions during the process and thus continuously changing the total electron dose that irradiated the area of interest. While this allowed for better imaging conditions by controlling the thickness of the liquid, the variation in the number of electrons impinging on the specimen can influence the link between the applied potential and the imaged degradation mechanisms. The authors reported that their observations showed a stable Pt nanoparticle size up to 200 cycles which then tripled in size but remained stable for the next 300 cycles. It was concluded that dissolution, reprecipitation, and coalescence by Oswald ripening occurred in parallel.

Overall, all ORR studies have focused on morphological stability insights, while the link between the onset of the degradation phenomena and the electrochemical inducing potential is difficult to establish.

3.1.3 *Dissolution, Reprecipitation, and Restructuring of Cu CO_2ER Catalysts*

In recent years, much research has been devoted to monitoring the degradation processes of Cu nanocatalysts for the CO_2ER using ec-LPTEM. Aran-Ais *et al*. used electrodeposited cubic CuO_2 particles and imaged their morphological changes in CO_2-saturated 0.1 M $KHCO_3$ (pH 7) at the reducing, uncalibrated potential of -0.7 V.[20] However, the interpretation and association of the changes with the CO_2ER effects were limited due to the use of structures with unknown activity or selectivity performance. Further morphology-based studies from the same group discussed similar effects in various systems.[21,22] Electrochemically tested Cu nanospheres were the focus of the experiments by Li *et al*.[23] which were performed at -0.6 V with respect to the internal reference electrode (*i.e*. less negative potential was used to avoid HER). They showed that 20 nm particles began to grow within fractions of a second. A more detailed study by Vavra *et al.*[24] using 7 nm Cu nanospheres, demonstrated the ability to perform the experiments at the more relevant potential of -0.8 V *vs* RHE by using in-house fabricated electrochemical chips with an extended inert window. Following a protocol of performing linear sweep voltammetry (LSV) and subsequent chronoamperometry (CA), they monitored the dissolution, reprecipitation, and growth of secondary particles, which took place by Ostwald ripening, while *operando* electron diffraction was also used to follow the change in structure from an initial Cu (II) to Cu (0) over the potential-induced cathodic process, Fig. 2c.

Overall, Cu nanocatalysts are an ideal system for the implementation of ec-LPTEM for monitoring morphological and structural changes, as long as appropriate electrochemical protocols are followed.

3.2 *Catalyst/Electrolyte Interactions*

Information about the way in which the liquid electrolyte interacts with the catalytic surfaces is essential for understanding the active sites. These interactions can be short-range (related to the formation of the electrical double layer, which ec-LPTEM cannot probe, as yet) and long-range (related to the total surface capacitance and charge distribution). Changes in these catalyst/electrolyte interactions are electrochemically-driven and precede the electrocatalytic reactions.

3.2.1 *Wetting Properties of Cobalt-Oxide OER Catalysts*

Shen *et al.* used TEM imaging to study the liquid-surface interactions of OER catalysts during CV measurements at pH 13.[14] By optimizing the functionalization of the substrate electrode, they were able to achieve thin liquid layer conditions whose formation around the cobalt-oxide particles could be switched during cycling between 1.0 V and 1.8 V *vs* RHE. They attributed the overall change in the liquid interaction with the surface to electrowetting and the voltage relationship to the capacitance of the oxide surface. Interestingly, the authors showed that the steep change in the wetting properties at 1.2 V *vs* RHE was related to the change in oxidation state and surface reconstruction of the surface spinel layer to the oxyhydroxide phase (Fig. 2d), a known active phase for OER metal-oxide catalysts. They also demonstrated that the process was fully reversible for the duration of their experiment, approximately for the first 15 cycles.

3.3 *Catalyst/Electrolyte/Gaseous Product Evolution*

The formation of gaseous products in TEM microcells during imaging of the electrocatalytic reactions is typically avoided for reasons related to imaging instabilities and potential microcell burst. However, the correlation of the gaseous products of heterogeneous electrocatalytic reactions with the applied stimuli and with the local surface sites of the catalyst has proven to be the most powerful diagnostic of ec-LPTEM.

3.3.1 *Spectroscopy for Product Detection in OER Catalysts*

To probe the evolved molecular oxygen from cobalt-oxide catalysts and confirm the activity of the dropcasted particles on the WE of the microcell, Shen *et al*. used electron energy loss spectroscopy (EELS) with a static electron beam parked near the particle surface.[14] A fingerprint pre-peak in the O K edge was probed above 1.65 V *vs* RHE., which was interpreted to correspond to the evolution of molecular oxygen, Fig. 2e. This process was also shown to be fully reversible. In a similar experiment, Shen *et al*. performed a two-dimensional EELS scan on the more robust IrO_2 and evaluated the evolution of molecular oxygen from the different facets of the particles.[18] It was shown that the molecular oxygen was probed in the liquid phase and its signal became progressively weaker away from the catalyst surface, while efforts to quantify this signal could be promising.[25] These results demonstrated the sensitivity of EELS measurements in detecting the product of the electrocatalytic reactions in the absence of any imaging contrast associated with gas or local bubble formation.

3.3.2 *Imaging H_2 Bubble Formation in MoS_2 During HER*

Kim *et al.* investigated the HER properties of MoS_2 flakes in acid (0.1 N H_2SO_4, pH 0.7).[26] They used a three-electrode system and applied a negative potential of up to -3.7 V *vs* RHE, while performing constant potential measurements to follow the bubble dynamics starting from their nucleation. Their results indicated that hydrogen bubble formation was influenced by the presence of various defects in the two-dimensional lattice, and their possible effects to the kinetics of HER were discussed. The authors reported that the bubble formation and evolution during the process disturbed liquid flow and electrolyte contact with the active sites of the catalyst, potentially inhibiting the local activity and continuous hydrogen evolution from the entire flake.

4. Outlook and Conclusion

There are many reasons for the paucity of *quasi-operando*-based TEM studies of electrocatalytic systems in liquids. Some of these have to do with the difficulty of dealing with the liquid and the inevitable electron scattering and radiolysis effects,[27] which can produce a background signal leading to one of two things; either the inhibition of the desired signal or the inability to follow the processes under realistic conditions and for their duration. Recognizing the limitations of microcell design for ec-TEM studies, particular attention should be paid to the following factors: 1) Appropriate substrates and calibrated stimuli are critical factors for mimicking realistic electrocatalytic conditions in the microcells. Recent advances in two-dimensional substrate electrodes combined with improvements in spatial resolution are promising;[28] 2) The effects of the electron beam in synergy with the applied potential require care in the choice of operating mode (transmission *vs* scanning transmission mode). A recent study has shown that diffusion transport of the radiolysis species in the liquid electrolytes is sufficient to replenish the electrolyte,[29] but the effect of the radiolysis products on the local pH cannot be excluded;[30] 3) The use of model catalysts is useful for calibrating the system. However, real catalysts whose activity and selectivity are determined electrochemically would be preferable to obtain meaningful ec-LPTEM results that can be related to their performance. Of course, coherence between the conditions of the bulk and microcell setups conditions remains a goal, especially since the as-synthesized non-noble metal and metal-oxide catalysts

undergo changes prior to the application of the electrochemical stimuli.[31]

In conclusion, as illustrated in Fig. 2a, there is a vast space to be explored with atypical signal acquisition and data analysis using *quasi-operando* ec-LPTEM applied to electrocatalysts. The power of TEM over other *operando* characterization techniques, lies in its ability to collect signals at the single particle level, which can provide information not only about the morphology and structure of the catalysts during operation, but also about the chemical environment and charge distribution at a very local scale. This unique combination of information obtained from a single characterization technique for surface and interfacial phenomena can unlock our fundamental understanding of the processes underlying the electrocatalytic systems in liquids.

Acknowledgements

The author thanks Jing Hou, Tzu-Hsien Shen, Jan Vavra, My Pham, Robin Girod, Morgan Binggeli, and Saltanat Toleukhanova for their valuable contributions to the understanding of electrochemical processes in microcells. This work was supported in part by the Swiss National Science Foundation under award nos. 200021_175711 and CRSII5_180335. This publication was created as part of NCCR Catalysis (grant number 180544), a National Centre of Competence in Research funded by the Swiss National Science Foundation.

Received: February 01, 2024

[1] B. M. Weckhuysen, *Chem. Soc. Rev.* **2010**, *39*, 4557, https://doi.org/10.1039/C0CS90031A.
[2] L. C. Liu, A. Corma, *Chem. Rev.* **2018**, *118*, 4981, https://doi.org/10.1021/acs.chemrev.7b00776.
[3] J. Hwang, R. R. Rao, L. Giordano, Y. Katayama, Y. Yu, Y. Shao-Horn, *Science* **2017**, *358*, 751, https://doi.org/10.1126/science.aam7092.
[4] C. Baeumer, *J. Appl. Phys.* **2021**, *129*, 170901, https://doi.org/10.1063/5.0046142.
[5] Y. Yang, Y. Xiong, R. Zeng, X. Y. Lu, M. Krumov, X. Huang, W. X. Xu, H. S. Wang, F. J. DiSalvo, J. D. Brock, D. A. Muller, H. D. Abruna, *ACS Cat.* **2021**, *11*, 1136, https://doi.org/10.1021/acscatal.0c04789.
[6] L. Negahdar, C. M. A. Parlett, M. A. Isaacs, A. M. Beale, K. Wilson, A. F. Lee, *Catal. Sci. Technol*. **2020**, *10*, 5362, https://doi.org/10.1039/d0cy00555j.
[7] M. A. Bañares, *Cat. Today* **2005**, *100*, 71, https://doi.org/10.1016/j.cattod.2004.12.017.
[8] T. H. Shen, R. Girod, V. Tileli, *Acc. Chem. Res*. **2023**, *56*, 3023, https://doi.org/10.1021/acs.accounts.3c00463.
[9] H. -Y. Chao, K. Venkatraman, S. Moniri, Y. Jiang, X. Tang, S. Dai, W. Gao, J. Miao, M. Chi, *Chem. Rev*. **2023**, *123*, 8347, https://doi.org/10.1021/acs.chemrev.2c00880.
[10] W. T. Hong, M. Risch, K. A. Stoerzinger, A. Grimaud, J. Suntivich, Y. Shao-Horn, *Energy Environ. Sci*. **2015**, *8*, 1404, https://doi.org/10.1039/C4EE03869J.
[11] S. Trasatti, O. A. Petrii, *Pure Appl. Chem*. **1991**, *63*, 711, https://doi.org/10.1351/pac199163050711.
[12] F. M. Ross, 'Liquid Cell Electron Microscopy', Cambridge University Press, Cambridge, **2016**.
[13] N. O. Pena, D. Ihiawakrim, M. Han, B. Lassalle-Kaiser, S. Carenco, C. Sanchez, C. Laberty-Robert, D. Portehault, O. Ersen, *ACS Nano*. **2019**, *13*, 11372, https://doi.org/10.1021/acsnano.9b04745.
[14] T. H. Shen, L. Spillane, J. Y. Peng, Y. Shao-Horn, V. Tileli, *Nat. Catal.* **2022**, *5*, 30, https://doi.org/10.1038/s41929-021-00723-w.
[15] S. E. Balaghi, S. Mehrabani, Y. Mousazade, R. Bagheri, A. S. Sologubenko, Z. L. Song, G. R. Patzke, M. M. Najafpour, *ACS Appl. Mat. Int.* **2021**, *13*, 19927, https://doi.org/10.1021/acsami.1c00243.
[16] G. Z. Zhu, S. Prabhudev, J. Yang, C. M. Gabardo, G. A. Botton, L. Soleymani, *J. Phys. Chem. C* **2014**, *118*, 22111, https://doi.org/10.1021/jp506857b.
[17] V. Beermann, M. E. Holtz, E. Padgett, J. F. de Araujo, D. A. Muller, P. Strasser, *Energy Environ. Sci.* **2019**, *12*, https://doi.org/10.1039/c9ee01185d.
[18] T. H. Shen, R. Girod, J. Vavra, V. Tileli, *J. Electrochem. Soc*. **2023**, *170*, https://doi.org/10.1149/1945-7111/acced4.
[19] A. Impagnatiello, G. Rizza, C. F. Cerqueira, P. E. Coulon, A. Morin, S. Escribano, L. Guetaz, M. C. Clochard, *ACS Appl. Energy Mat.* **2020**, *3*, 2360, https://doi.org/10.1021/acsaem.9b02000.
[20] R. M. Aran-Ais, R. Rizo, P. Grosse, G. Algara-Siller, K. Dembel, M. Plodinec, T. Lunkenbein, S. W. Chee, B. Roldan Cuenya, *Nat. Comm*. **2020**, *11*, https://doi.org/10.1038/s41467-020-17220-6.
[21] P. Grosse, A. Yoon, C. Rettenmaier, A. Herzog, S. W. Chee, B. R. Cuenya, *Nat. Comm*. **2021**, *12*, https://doi.org/10.1038/s41467-021-26743-5.
[22] A. Yoon, J. Poon, P. Grosse, S. W. Chee, B. Roldan Cuenya, *J. Mat. Chem. A* **2022**, *10*, 14041, https://doi.org/10.1039/d1ta11089f.
[23] Y. Li, D. Kim, S. Louisia, C. Xie, Q. Kong, S. Yu, T. Lin, S. Aloni, S. C. Fakra, P. Yang, *Proc. Natl. Acad. Sci. USA* **2020**, *117*, 9194, https://doi.org/10.1073/pnas.1918602117.
[24] J. Vavra, T. H. Shen, D. Stoian, V. Tileli, R. Buonsanti, *Angew. Chem. Int. Ed.* **2021**, *60*, 1347, https://doi.org/10.1002/anie.202011137.
[25] T. H. Shen, V. Tileli, *Microsc. Microanal*. **2022**, *22*, 812 https://doi.org/10.1017/S1431927622003646.
[26] J. Kim, A. Park, J. Kim, S. J. Kwak, J. Y. Lee, D. Lee, S. Kim, B. K. Choi, S. Kim, J. Kwag, Y. Kim, S. Jeon, W. C. Lee, T. Hyeon, C.-H. Lee, W. B. Lee, J. Park, *Adv. Mat.* **2022**, *34*, 2206066, https://doi.org/10.1002/adma.202206066.
[27] N. M. Schneider, M. M. Norton, B. J. Mendel, J. M. Grogan, F. M. Ross, H. H. Bau, *J. Phys. Chem. C* **2014**, *118*, 22373, https://doi.org/10.1021/jp507400n.
[28] S. Toleukhanova, T.-H. Shen, C. Chang, S. Swathilakshmi, T. Bottinelli Montandon, V. Tileli, *Adv. Mat*. **2024**, 2311133, https://doi.org/10.1002/adma.202311133.
[29] S. Merkens, G. De Salvo, A. Chuvilin, *Nano Express* **2022**, *3*, 045006, https://doi.org/10.1088/2632-959X/acad18.
[30] T. Couasnon, B. Fritsch, M. P. M. Jank, R. Blukis, A. Hutzler, L. G. Benning, *Adv. Sci.* **2023**, *10*, 2301904, https://doi.org/10.1002/advs.202301904.
[31] D. Hochfilzer, I. Chorkendorff, J. Kibsgaard, *ACS Energy Lett.* **2023**, *8*, 1607, https://doi.org/10.1021/acsenergylett.3c00021.